Solvothermal Synthesis of V−VI Binary and Ternary Hexagonal Platelets: The Oriented Attachment Mechanism

ARTICLE *in* CRYSTAL GROWTH & DESIGN · NOVEMBER 2008

Impact Factor: 4.89 · DOI: 10.1021/cg7012528

4 AUTHORS, INCLUDING:

Wei Wang
Ocean University of China
1,003 PUBLICATIONS **15,926** CITATIONS

SEE PROFILE

Xiaoli Lu
Xidian University
30 PUBLICATIONS **456** CITATIONS

SEE PROFILE

Xiaoguang Li
University of Science and Technology of C…
297 PUBLICATIONS **3,887** CITATIONS

SEE PROFILE

CRYSTAL GROWTH & DESIGN
2009
VOL. 9, NO. 1
145–150

Solvothermal Synthesis of V−VI Binary and Ternary Hexagonal Platelets: The Oriented Attachment Mechanism

Genqiang Zhang, Wei Wang, Xiaoli Lu, and Xiaoguang Li*

Hefei National Laboratory for Physical Sciences at Microscale, Department of Physics, University of Science and Technology of China, Hefei 230026, P. R. China, and the International Center for Materials Physics Academia Sinica, Shenyang 110015, P. R. China

Received December 20, 2007; Revised Manuscript Received September 11, 2008

ABSTRACT: General synthesis of both binary and ternary V−VI based thermoelectric alloy hexagonal platelets was carried out for the first time in a unified system using a modified solvothermal method, which adopted convenient oxides as source materials and friendly ethylene glycol as both solvent and reducing agent. The structure and composition analysis reveal that the samples are pure phase with corresponding atomic ratios. Electron microscopy results indicate that the as-prepared products are uniform and highly crystallized. The formation process was studied in detail by observing time-dependent products, and it was found that the oriented attachment mechanism could be responsible for the growth of these hexagonal platelets, which exhibits intrinsic difference compared with the inferred seed-mediated growth mechanism in previous reports. The influence of pH value and polyvinyl pyrrolidone on the morphology of the products was investigated as well. This work may open up a new rationale on designing the solution synthesis of nanostructures for materials possessing similar intrinsic crystal symmetry.

1. Introduction

Because $A_2^VB_3^{VI}$-type compounds, such as Bi_2Te_3, Sb_2Te_3, Bi_2Se_3, and their ternary alloys, including Bi−Te−Se, and Bi−Sb−Te, are of great interest and significance for potential applications in thermoelectric convertors,[1−4] considerable efforts have been devoted to synthesize this type of compound with controllable sizes and morphologies. Examples include the following: (i) for zero-dimensional nanocrystals, well-crystallized Bi_2Te_3 and $Bi_{0.5}Sb_{1.5}Te_3$ nanoparticles have been obtained through the microemulsion method and ball milling process;[5,6] (ii) for one-dimensional nanomaterials, Bi_2Te_3 nanorods/tubes,[7−9] Sb_2Te_3 nanobelts,[10] and a group of $A_2^VB_3^{VI}$ and related heterostructure nanowire arrays[11−18] were successfully synthesized by the solution phase method, hydro/solvo-thermal process, and electrodeposition combined with porous anodic alumina template method; (iii) while for the two-dimensional (2D) platelet-like structure, though limited reports demonstrated that hexagonal Bi_2Te_3, Bi_2Se_3, and Sb_2Te_3 nano/microplates could be obtained using the high-temperature organic solution approach and the solvo/hydro-thermal process, respectively,[19−21] it is still a challenge to search general and facile routes to synthesize both binary and ternary $A_2^VB_3^{VI}$-type platelet-like structures.

Considering that $A_2^VB_3^{VI}$-type compounds have similar crystal symmetry and an anisotropic bonding environment,[22−24] it is possible to build this class of materials into 2D platelet-like morphology in a unified system. Herein, we develop a simple solvothermal approach using convenient oxides as source materials and nontoxic ethylene glycol as reducing agent, which is feasible to synthesize high-quality $A_2^VB_3^{VI}$-type alloy hexagonal platelets. By analyzing products of Bi_2Te_3 with different reaction time, it can be deduced that this general route involves the oriented attachment mechanism during the hexagonal platelets formation. In this case, it should be appropriate for obtaining ternary V−VI alloys because they have an intrinsic crystal structure similar to that of binary alloys. Two selected ternary hexagonal platelets were successfully prepared by the above-mentioned method. This work may provide a new rationale pertaining to the design of the solution synthesis of nanoarchitectures for materials possessing similar intrinsic crystal symmetry.

2. Experimental Section

Analytical grade Bi_2O_3, Sb_2O_3, TeO_2, SeO_2, ethylene glycol, polyvinyl pyrrolidone (PVP, K-30, $M_s \approx 40\,000$), and NaOH were used without further purification. The reaction was carried out in a 25-mL Teflon-lined stainless-steel autoclave, and the temperature was regulated by a digital-type temperature-controlled oven.

The typical procedure for the synthesis of Bi_2Te_3 nanoplates is as follows: 0.4 g PVP was dissolved in ethylene glycol (18 mL) to form a clear solution, followed by the addition of Bi_2O_3 (0.2298 g, 0.5 mmol), TeO_2 (0.2394 g, 1.5 mmol), and 2 mL of NaOH solution (4 mol/L). The resulting precursor suspension was stirred vigorously for 30 min, and then sealed in the autoclave. The autoclave was then heated to and maintained at 200 °C for 4 h. The products were collected by centrifugation, washed several times with distilled water and absolute ethanol, and finally dried in a vacuum at 60 °C. The above process can be extended to the synthesis of other binary and ternary $A_2^VB_3^{VI}$-type micro/nanoplates by adjusting the NaOH concentration and reaction time.

The crystal structure of the as-prepared products was characterized by X-ray diffraction (XRD), recorded on a Philips X'Pert Pro Super X-ray diffractometer equipped with graphite monochromatized, Cu Kα radiation ($\lambda = 1.54178$ Å). Field-emission scanning electron microscopy was applied to investigate the size and morphology, which was carried out with a field emission electron microanalyzer (JEOL 6700F). Electron microscopy analyses were performed on a Hitachi H-800 transmission electron microscope (TEM) and JEOL-2010 high-resolution TEM, at an acceleration voltage of 200 kV.

3. Results and Discussion

Typical syntheses of both binary and ternary $A_2^VB_3^{VI}$-type hexagonal platelets were carried out in a solvothermal system based on the modified reduction reaction between oxides and ethylene glycol (EG).[25,26] The morphology of the Bi_2Te_3 nanoplates obtained at 200 °C for 4 h with NaOH concentration of 0.5 mol/L is shown in Figure 1a−d, and all the platelets exhibit uniform hexagonal shapes on top−bottom facets. The low-magnification scanning electron microscopy (SEM) image shown in Figure 1a indicates the high-yield growth feature of this simple solvothermal process. The edge length and thickness

* To whom correspondence should be addressed. Tel./Fax: 86-551-3603408. E-mail: lixg@ustc.edu.cn.

10.1021/cg7012528 CCC: $40.75
Published on Web 11/26/2008

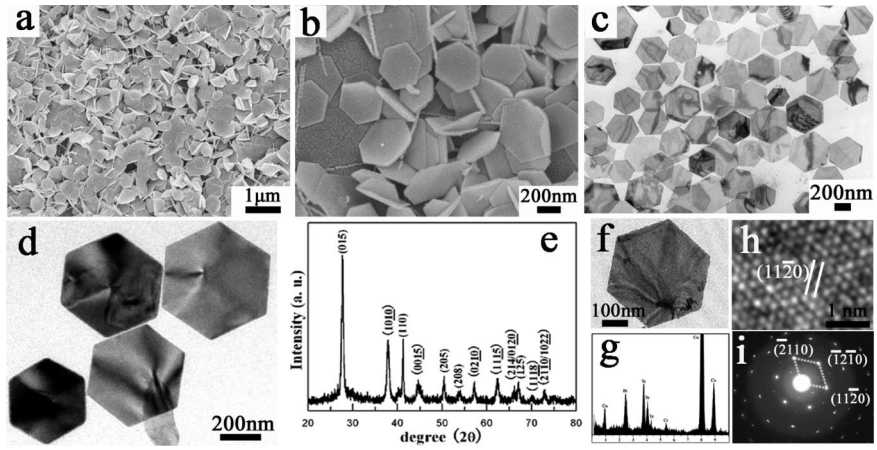

Figure 1. Integrated characterization of Bi_2Te_3 nanoplates obtained at 200 °C for 4 h with NaOH concentration of 0.5 mol/L and 0.4 g PVP: (a, b) SEM and (c, d) TEM images in different magnifications; (e) typical XRD pattern; (f) TEM image of an individual hexagonal plate; (g) EDS spectrum, (h) HRTEM image, (i) ED pattern carried on the plate in panel f.

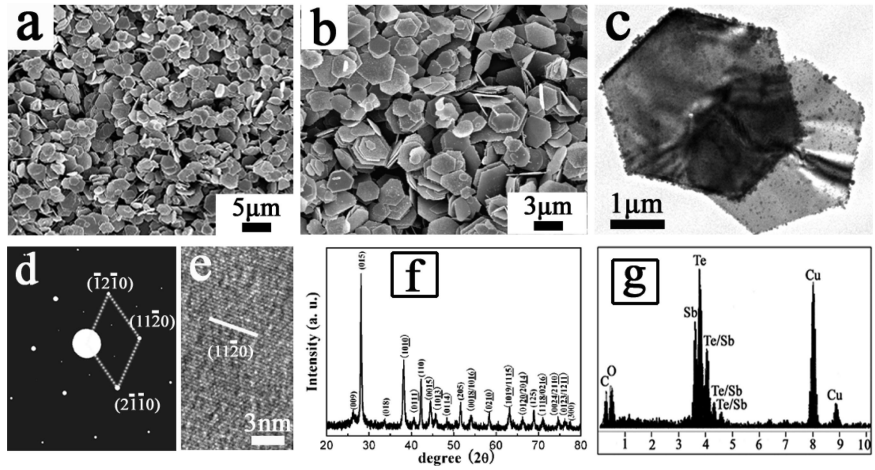

Figure 2. (a, b) SEM and (c) TEM images; (d) ED pattern; (e) HRTEM image; (f) XRD pattern; and (g) EDS spectrum of the Sb_2Te_3 hexagonal microplates obtained at 200 °C for 16 h with NaOH concentration of 0.9 mol/L and 0.4 g PVP.

of the nanoplates, estimated from Figure 1b, are 240∼320 nm and 30∼40 nm, respectively. Figure 1c,d gives the typical transmission electron microscopy (TEM) images of the nanoplates in different magnifications, which indicate the good uniformity of the sample. The X-ray diffraction (XRD) pattern, as shown in Figure 1e, can be steadily indexed to rhombohedral Bi_2Te_3 structure (JCPDS Card Number 82-0358, $R\bar{3}m$). The energy-dispersive X-ray spectroscopy (EDS) spectrum (Figure 1g) exhibits that besides the Cu, C, and Cr signals arising from the use of copper grid, only peaks of the elements Bi and Te are presented with an approximate atomic ratio of 2:3, which is consistent with the stoichiometry of Bi_2Te_3. The high-resolution TEM (HRTEM) image (Figure 1h) and selected area electron diffraction (SAED) pattern (Figure 1i) performed on the single hexagonal nanoplate shown in Figure 1f exhibit clear lattice fringes and hexagonally symmetric spots pattern, respectively, indicating that the nanoplates are highly crystallized and defect-free. The SAED pattern can be assigned to [0001] zone axis projection of the hexagonal Bi_2Te_3 reciprocal lattice, and the spacing of the adjacent fringes shown in Figure 1h corresponds to the $(11\bar{2}0)$ planes of the Bi_2Te_3. The results indicate that the top−bottom surfaces are {0001} facets while six side surfaces should be $\{11\bar{2}0\}$ facets, and the growth direction for developing the hexagon morphology is $\langle 11\bar{2}0\rangle$ direction, which is consistent with the previous report.[16]

To examine the generality of this solvothermal route, the synthesis of Sb_2Te_3 and Bi_2Se_3 nanostructures was also studied in detail. In previous literature, Ren et al.[20] reported the first synthesis of Sb_2Te_3 hexagonal platelets using $N_2H_4 \cdot H_2O$ as reducing agent and cetyltrimethylammonium (CTAB) as surfactant under solvothermal condition. However, the size distribution is relatively broad—from 200 to 2000 nm, and the existed impurity of element Te may play a negative role in further investigation on the thermoelectric properties. Using the general route in this work, uniform and impurity-free Sb_2Te_3 hexagonal plates with average edge lengths of ∼2 μm, as shown in Figure 2a−c, can be obtained. The microstructure analyses (Figure 2d−f) indicate that the as-prepared product is pure phase and single crystalline. The EDS spectrum shown in Figure 2g reveals the stoichiometry of the Sb_2Te_3. In addition, ultrathin Bi_2Se_3 hexagonal microplates can also be obtained under conditions similar to that of the Bi_2Te_3 synthesis. Electron microscopy analyses (see Supporting Information, Figure S1) show that the average edge lengths of the platelets are 4∼5 μm and the thickness is estimated to be less than 5 nm.

The syntheses of two selected ternary V−VI based alloys—Bi_2Te_2Se and $BiSbTe_3$ hexagonal platelets—through the general route mentioned above were performed to demonstrate the feasibility of further extending this simple solvothermal approach. Figure 3 shows the morphology observation and

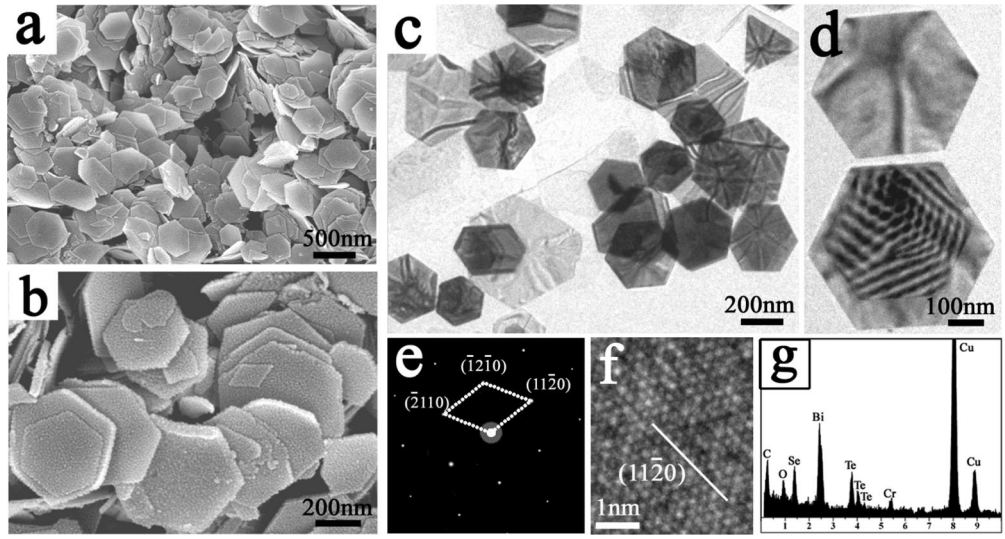

Figure 3. Characterization of the Bi_2Te_2Se nanoplates obtained at 200 °C for 10 h with a NaOH concentration of 0.5 mol/L and 0.4 g PVP: (a, b) typical SEM and (c, d) TEM images; (e) SAED pattern; (f) HRTEM image; (g) EDS spectrum.

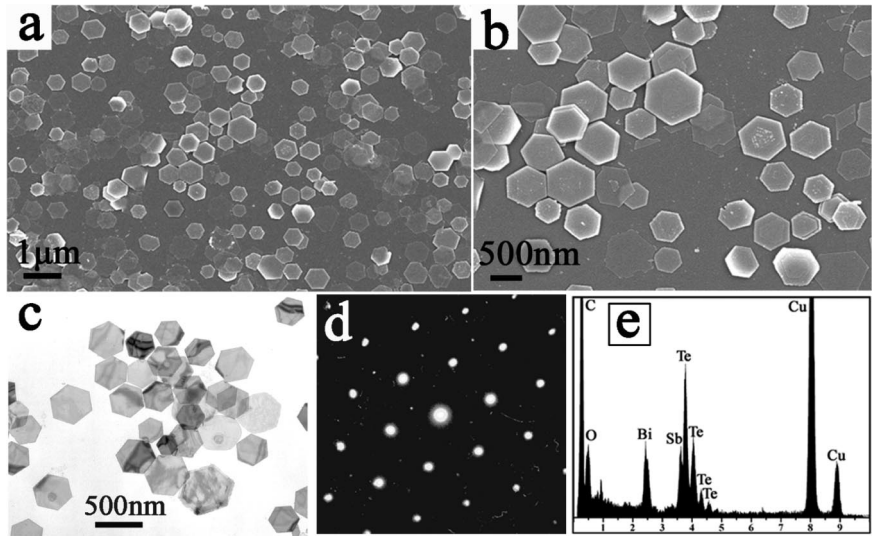

Figure 4. $BiSbTe_3$ hexagonal platelets obtained at 200 °C for 20 h with NaOH concentration of 0.9 mol/L and 0.4 g PVP: (a, b) SEM images in different magnifications; (c) typical TEM image; (d) ED pattern; and (e) EDS spectrum.

microstructure analyses of Bi_2Te_2Se obtained at 200 °C for 10 h with NaOH concentration of 0.9 mol/L. Both the SEM and TEM images, as shown in Figure 3a−d, demonstrate that high-quantity synthesis of uniform Bi−Te−Se alloy hexagonal platelets can be routinely accomplished. The edge length and thickness are about 200∼300 and 25 nm, respectively. The typical XRD pattern (see Supporting Information, Figure S2) of the as-prepared Bi_2Te_2Se platelets can be identified as rhombohedral structures with space group of $R\bar{3}m$ (JCPDS Card Number 29-0247). Both the the SAED pattern (Figure 3e) and HRTEM image (Figure 3f) reveal the well-crystallized and defect-free feature of the product, which are similar to those of Bi_2Te_3 platelets. The corresponding EDS spectrum shown in Figure 3g reveals the atomic ratio of the involving elements: Bi, Te, and Se, which is 2.33:2.03:1.00, presenting slight deviation from the corresponding nominal stoichiometry, due possibly to the formation of antisite Bi defects in Te or Se sites.[27]

For the synthesis of $BiSbTe_3$ hexagonal platelets, the reaction time needs to be increased to 20 h in order to obtain its pure phase. The as-prepared product exhibits the high-yield growth and well crystallization, as shown in Figure 4a−c. The edge length and thickness are estimated to be 280∼360 nm and about 40 nm, respectively. The SAED pattern (Figure 4d) analogous to others indicates its single crystalline nature. EDS spectrum shown in Figure 4e indicates that the as-prepared product is pure phase with an approximate stoichiometry of 1:1:3.

It can be concluded that, using this facile and unified solvothermal method, both binary and ternary $A_2^VB_3^{VI}$-type hexagonal nano/microplatelets can be successfully synthesized. The results also demonstrate that the atomic ratios of the involving elements are tunable, which allows the possibility of searching materials possessing optimized thermoelectric performance.

In order to comprehensively understand this general method, the formation process of the hexagonal platelet structure is studied in detail. In previous literature,[19,20] it was believed that the formation of platelet-like morphology of $A_2^VB_3^{VI}$-type alloys should be related to their inherently anisotropic bonding environment, resulting in much faster growth along the top−bottom crystalline planes than along the *c*-axis. However,

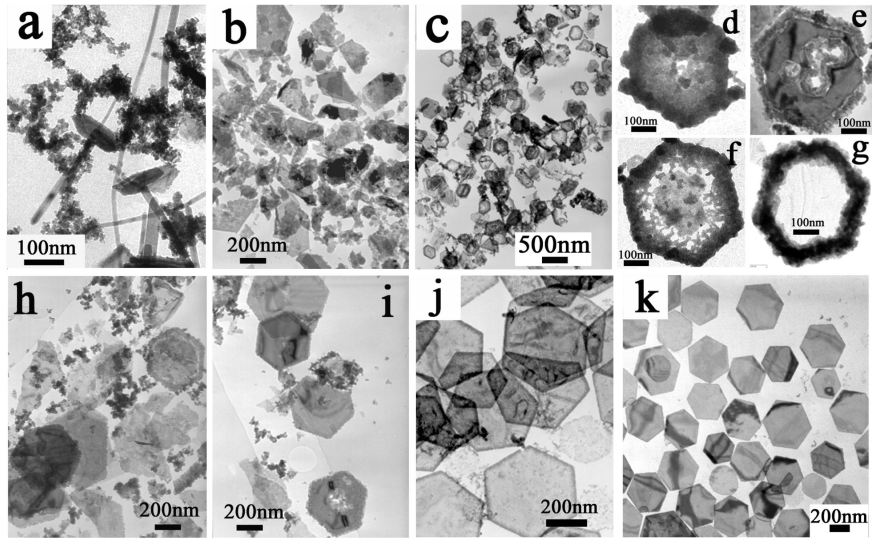

Figure 5. TEM images of the time-dependent morphologies of Bi_2Te_3 at 200 °C with NaOH concentration of 0.5 mol/L and 0.4 g PVP: (a) 20; (b) 60; (c-i) 100; (j) 160; and (k) 240 min.

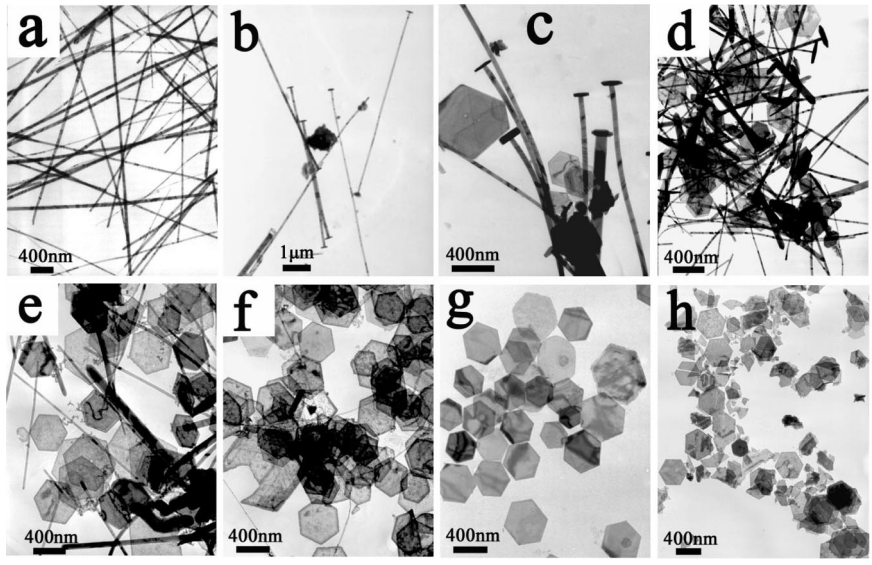

Figure 6. TEM images of the products obtained using Bi_2O_3 and TeO_2 as source materials and 0.4 g PVP as stabilizing agent with different NaOH concentrations at 200 °C for 4 h: (a) 0; (b) 0.1; (c) 0.2; (d) 0.25; (e) 0.3; (f) 0.4; (g) 0.5; (h) 1.5 mol/L.

the specific growth process remains an unambiguous topic though it is inferred that the primary platelet seed induced process may be the possible mechanism.[19,20] Therefore, time-dependent morphologies of Bi_2Te_3 are carefully observed as an example (Figure 5) in order to disclose the formation process, and the "oriented attachment" mechanism [23,28−31] is found to be responsible for the growth of Bi_2Te_3 hexagonal platelets. The stepwise formation process is described as follows: The Bi nanocrystals and Te nanowires are first produced by reducing Bi_2O_3 and TeO_2 with the EG at elevated temperature.[25,26] Figure 5a gives the typical TEM image of the products obtained at 200 °C for 20 min. Te nanowires, irregular Bi−Te alloy nanocrystals with atomic ratio of about 4:1 (see Supporting Information, Figure S3), and a few Bi−Te alloy platelets are found. At the early stage, three kinds of processes involved in this solvothermal route—(i) the formation of Bi nanocrystals and Te nanowires, (ii) the dissolving and subsequently fusing of Bi and Te crystals into Bi−Te alloy nanoparticles, and (iii) the oriented attachment of the alloy particles into hexagonal Bi_2Te_3 nanoplates through recrystallization—happened in an ordered sequence and should coexist for a short stage, which results in the multiple morphologies as shown in Figure 5a.

When the reaction time reaches 60 min, only Bi_2Te_3 platelet-like fractions together with a small proportion of regular hexagonal nanoplates (Figure 5b) are observed. This result indicates that the alignment of Bi−Te alloy nanocrystals into platelet-like morphology is the dominant process during this stage. Along with the reaction time prolonged to 100 min, most of the Bi_2Te_3 platelet-like fractions have developed into hexagonally shaped platelets as shown in Figure 5c, and the correspondingly magnified TEM images of three kinds of typical platelets shown in Figure 5d−f reveal that most of the platelets exhibit rough external hexagonal frames followed by the relatively well-crystallized inner hexagonal spaces. Interestingly, very few individual hexagonal nanorings are observed, and a typical TEM image is shown in Figure 5g. This may be due to the post treatment which shakes off the inner space. Also, there are still a few platelet fractions and well-crystallized hexagonal

platelets as demonstrated in panels h and i of Figure 5, respectively. The multiple morphologies in this stage reveal that the well-crystallized platelets experience particle alignment followed by the subsequent oriented attachment process.

By carefully observing HRTEM images of these nanoplates (see Supporting Information, Figure S4), it can be seen that the inner space of platelets exhibits single crystalline nature, illustrating the accomplishment of oriented alignment of the particles in the {0001} plane along the $\langle 11\bar{2}0\rangle$ direction, while the external hexagonal frame is still polycrystalline. Figure S5 (see Supporting Information) gives the HRTEM images of another selected platelet, and the result indicates that the oriented attachment process of the hexagonal frame is in progress. The formation of hexagonal frame should be due to the intrinsic hexagonal symmetry of the involved Bi_2Te_3 particles.[20] When the reaction time reaches 160 min, the hexagonal nanoplates shown in Figure 5j have been the dominated products, and the HRTEM images taken from two randomly selected platelets (see Supporting Information, Figure S6) demonstrate that the external hexagonal frames also show a single crystalline nature, indicating the formation of whole single crystalline hexagonal platelets. The product further develops into highly crystallized platelets after being kept at the settled temperature for 240 min (Figure 5k).

The concluded formation of the Bi_2Te_3 nanoplates may include four steps: (i) reduction of Bi_2O_3 and TeO_2 by EG; (ii) dissolving of Bi and Te crystals and the subsequent formation of Bi−Te alloy particles; (iii) oriented attachment of the Bi−Te alloy particles into hexagonal platelets consisting of single crystalline inner spaces terminated by polycrystalline hexagonal frames, and (iv) the formation of whole single crystal hexagonal platelets after the hexagonal frames evolve into single crystalline through oriented attachment.

In order to further investigate this general solvothermal method, the influence of NaOH concentration and polyvinyl pyrrolidone (PVP) on the morphology was investigated as well. Figure 6 shows the typical TEM images of the products obtained after aging at 200 °C for 4 h with different NaOH concentrations (Figure 6a, 0; b, 0.1; c, 0.2; d, 0.25; e, 0.3; f, 0.4; g, 0.5; h, 1.5 mol/L). Only uniform nanowires (Figure 6a) with average diameters of about 50 nm were obtained if no NaOH was added to the solvent. The SAED pattern and EDS spectrum (see Supporting Information, Figure S7) indicate that the products are pure Te.

Interestingly, the "I" shaped Te nanowires were observed with NaOH concentration of 0.1 mol/L (Figure 6b). EDS analysis (see Supporting Information, Figure S8) indicates that the platelets connected to both ends of the Te nanowires was Bi−Te alloys with atomic ratio of ∼1:2. With the further increased amount of NaOH to 0.2 mol/L, some regularly hexagonal nanoplates emerged besides the "I" shaped Te nanowires (Figure 6c). The proportion of hexagonal nanoplates gradually increased with the increasing NaOH concentrations (Figure 6d−f), and pure hexagonal platelets with highly crystallized feature, as shown in Figure 6g, were obtained when the NaOH concentration reached 0.5 mol/L. However, an ultrahigh NaOH concentration could play a negative role in the hexagonal morphology. Figure 6h exhibited the product obtained with the NaOH concentration of 1.5 mol/L, and the result indicates that many of the hexagonal platelets have cracked into irregular fractions. It can be seen that the amount of NaOH plays a critical role in determining the morphology of the product, and it is necessary to add an appropriate amount of NaOH in order to obtain pure, highly crystallized Bi_2Te_3 hexagonal platelets at a settled temperature and reaction time.

On the other hand, the aging time also drastically decides the morphology of the product. For example, when the NaOH concentration is 0.3 mol/L, the product collected at 200 °C for 12 h was pure Bi_2Te_3 nanoplates while only the mixture of Te wires and some Bi−Te alloy hexagonal platelets could be obtained (Figure 6e) when the reaction time is only 4 h. Therefore, it can be concluded that the initial NaOH concentration of the precursor medium strongly influences the reaction rate of the three reactions mentioned above during the formation of Bi_2Te_3 alloy, especially the dissolving of Te nanowires and subsequent recrystallization into Bi−Te alloy. This will lead to the existence of Te nanowires for a relatively longer time in the system with lower NaOH concentrations compared with those having higher concentrations. The role of PVP for the formation of Bi_2Te_3 hexagonal platelets was concluded as a stabilizing agent and size focusing additive by examining the morphology of the products obtained without PVP and by replacing PVP with equivalent CTAB (see Supporting Information, Figures S9 and S10).

4. Conclusion

In summary, a facile and general solvothermal process was developed to synthesize hexagonal platelets of several $A_2^{V}B_3^{VI}$-type alloys using ethylene glycol as both solvent and reducing agent and using PVP as a stabilizing agent. The formation process of the plate-like structure has been investigated in detail, and it is found that the oriented attachment mechanism clearly contributes to the creation of this structure. The influence of NaOH concentration and surfactant on the morphology is studied as well. This powerful route demonstrates that it is possible to obtain well-defined hexagonal plates of both binary and ternary $A_2^{V}B_3^{VI}$-type alloys with tunable atomic ratios by a modified reduction reaction using convenient oxides as precursors, which could be further extended to design the morphologies of other inorganic crystals.

Acknowledgment. This work was supported by the National Natural Science Foundation of China (50721061 and 50772111) and the National Basic Research Program of China (2006CB922005 and 2006CB929502).

Supporting Information Available: This material is available free of charge via the Internet at http://pubs.acs.org.

References

(1) Venkatasubramaniam, R.; Siivola, E.; Colpitts, T.; Quinn, B. O. *Nature* **2001**, *413*, 597.
(2) Wright, D. A. *Nature* **1958**, *181*, 834.
(3) Polvani, D. A.; Meng, I. E.; Chandrashekar, N. V.; Sharp, I.; Radding, I. V. *Chem. Mater.* **2001**, *13*, 2068.
(4) Harman, T. C.; Taylor, P. J.; Walsh, M. P.; LaForge, B. E. *Science* **2002**, *297*, 2229.
(5) Qiu, X. F.; Austin, L. N.; Muscarella, P. A.; Dyck, J. S.; Burda, C. *Angew. Chem., Int. Ed.* **2006**, *45*, 5655.
(6) Poudel, B.; Hao, Q.; Ma, Y.; Lan, Y. C.; Minnich, A.; Yu, B.; Yan, X.; Wang, D. Z.; Muto, A.; Vashaee, D.; Chen, X. Y.; Liu, J. M.; Dresselhous, M. S.; Chen, G.; Ren, Z. F. *Science* **2008**, *320*, 634.
(7) Purkayasha, A.; Lupo, F.; Kim, S. Y.; Borca-Tasciuc, T.; Ramanath, G. *Adv. Mater.* **2006**, *18*, 496.
(8) Zhao, X. B.; Ji, X. H.; Zhang, Y. H.; Zhu, T. J.; Tu, J. P.; Zhang, X. B. *Appl. Phys. Lett.* **2005**, *86*, 062111.
(9) Xiao, F.; Yoo, B. Y.; Lee, K. H.; Myung, N. V. *J. Am. Chem. Soc.* **2007**, *129*, 10068.
(10) Shi, W. D.; Yu, J. B.; Wang, H. S.; Zhang, H. J. *J. Am. Chem. Soc.* **2006**, *128*, 16490.

(11) Martin-Gonzalez, M.; Prieto, A. L.; Gronsky, R.; Sands, T.; Stacy, A. M. *Adv. Mater.* **2003**, *15*, 1003.
(12) Prieto, A. L.; Sander, M. S.; Martin-Gonzalez, M. S.; Gronsky, R.; Sands, T.; Stacy, A. M. *J. Am. Chem. Soc.* **2001**, *123*, 7160.
(13) Xiao, F.; Yoo, B. Y.; Lee, K. H.; Myung, N. V. *Nanotechnology* **2007**, *18*, 325203.
(14) Lim, J. R.; Whitacre, J. F.; Fleurial, J. P.; Huang, C. K.; Ryan, M. A.; Myung, N. V. *Adv. Mater.* **2005**, *17*, 1492.
(15) Yoo, B. Y.; Xiao, F.; Bozhilov, K. N.; Herman, J.; Ryan, M. A.; Myung, N. V. *Adv. Mater.* **2007**, *19*, 296.
(16) Wang, W.; Lu, X. L.; Zhang, T.; Zhang, G. Q.; Jiang, W. J.; Li, X. G. *J. Am. Chem. Soc.* **2007**, *129*, 6702.
(17) Jin, C. G.; Zhang, G. Q.; Qian, T.; Li, X. G.; Yao, Z. *J. Phys. Chem. B* **2005**, *106*, 1430.
(18) Zhou, J. H.; Jin, C. G.; Seol, J. H.; Li, X. G.; Shi, L. *Appl. Phys. Lett.* **2005**, *87*, 133109.
(19) Lu, W. G.; Ding, Y.; Chen, Y. X.; Wang, Z. L.; Fang, J. Y. *J. Am. Chem. Soc.* **2005**, *127*, 10112.
(20) Wang, W. Z.; Poudel, B.; Yang, J.; Wang, D. Z.; Ren, Z. F. *J. Am. Chem. Soc.* **2005**, *127*, 13792.
(21) Wang, D. B.; Yu, D. B.; Mo, M. S.; Liu, X. M.; Qian, Y. T. *J. Cryst. Growth* **2003**, *253*, 445.
(22) Wang, X.; Zhuang, J.; Peng, Q.; Li, Y. D. *Nature* **2005**, *437*, 121.
(23) Liu, B.; Zeng, H. C. *J. Am. Chem. Soc.* **2005**, *127*, 18262.
(24) Deng, H.; Li, X. L.; Peng, Q.; Wang, X.; Chen, J. P.; Li, Y. D. *Angew. Chem., Int. Ed.* **2005**, *44*, 2782.
(25) Liu, X. Y.; Zeng, J. H.; Zhang, S. Y.; Zheng, R. B.; Liu, X. M.; Qian, Y. T. *Chem. Phys. Lett.* **2003**, *374*, 348.
(26) Mayers, B.; Xia, Y. N. *J. Mater. Chem.* **2002**, *12*, 1875.
(27) Miller, G. R.; Li, C. Y. *J. Phys. Chem. Solids* **1965**, *26*, 3.
(28) Tang, Z.; Kotov, N. A.; Giersig, M. *Science* **2002**, *297*, 237.
(29) Pachiolski, C.; Kornowski, A.; Weller, H. *Angew. Chem., Int. Ed.* **2002**, *41*, 1188.
(30) Korgel, B. A.; Fitzmaurice, D. *Adv. Mater.* **1998**, *10*, 661.
(31) Cho, K. S.; Talapin, D. V.; Gaschler, W.; Murray, C. B. *J. Am. Chem. Soc.* **2005**, *127*, 7140.

CG7012528